



J. Serb. Chem. Soc. 78 (11) 1797–1807 (2013)
JSCS–4534

Investigation of the charge-transfer in photo-excited nanoparticles for CO₂ reduction in non-aqueous media[•]

NADA M. DIMITRIJEVIĆ*

*Chemical Sciences and Engineering Division, and Nanoscience and Technology Division,
Argonne National Laboratory, 9700 S. Cass Ave., Argonne, IL 60439, USA*

(Received 26 July, revised 19 September 2013)

Abstract: Photo-induced charge separation in TiO₂ and Cu₂O semiconductor nanoparticles was examined using electron paramagnetic resonance spectroscopy in order to obtain insight into the photocatalytic reduction of CO₂ in non-aqueous media. For dissolution/grafting of CO₂, carboxy-PEG₄-amine was used with poly(ethylene glycol) 200 as the solvent. It was found that the reduction of CO₂ in this system starts at a potential of –0.5 V vs. Ag/AgCl, which is significantly more positive than the potential for electrochemical reduction of CO₂ in most organic solvents and water (–2.0 V vs. Ag/AgCl). The electron transfer from excited nanoparticles to CO₂ is governed by both thermodynamic and kinetic parameters, namely by the redox potential of conduction band electrons and adsorption/binding of CO₂ on the surface of the nanoparticles.

Keywords: carbon dioxide reduction, photocatalysis, titanium dioxide, cuprous oxide.

INTRODUCTION

Carbon dioxide produced by consuming fossil fuels is regarded as the most significant source of greenhouse gases.¹ Reducing the accumulation of CO₂ in the atmosphere is one of the current major scientific and social challenges. Although the chemical industry currently uses CO₂ as an inexpensive, non-flammable and non-toxic C₁ resource, the processes are conducted at relatively high pressures, at elevated temperatures and in the presence of catalysts.^{2–6} Thus, there is a need for the development of facile and inexpensive methods to convert CO₂ to usable materials under mild conditions (temperature and pressure). Using solar light as an energy source and inexpensive semiconductor nanoparticles as photocatalysts is a promising approach for the photochemical transformation of

* Correspondence to E-mail: Dimitrijevic@anl.gov

[•] Dedicated to late Dr. Olga Mičić, the greatest teacher of Physical Chemistry.

doi: 10.2298/JSC130726093D

CO₂ into fuels: CO, CH₄, and CH₃OH. Each of these fuels could be burned to produce CO₂ and then regenerated by photochemical reduction. Alternatively, CO could be used as a starting material in the water gas shift reaction to generate hydrogen from water. In all these cases, energy would be produced in a CO₂ neutral fashion avoiding a net production of CO₂. While most semiconductor-assisted photocatalytic reductions of CO₂ were realized in aqueous solution,^{7–10} the yields were relatively low not only because of the low solubility of carbon dioxide in water, but also because adsorbed/dissociated water on the surface of nanoparticles competes with adsorbed CO₂ for the photogenerated electrons.¹¹ Different strategies in improving CO₂ sequestration are currently being pursued. Several groups^{12–14} have developed reversible CO₂ capture utilizing a strong nitrogen-containing base in conjunction with a proton donor. Meanwhile, amidophosphoranes were also proved to be capable of capturing one equivalent of CO₂ through the insertion of CO₂ into a P–N bond, resulting in the generation of carbamatophosphoranes.¹⁵ Very recently, Brennecke and co-workers¹⁶ designed an ionic liquid (IL) comprising an amino-functionalized anion and a long-chain alkyl phosphonium cation to capture CO₂, while Liu¹⁷ *et al.* employed poly(ethylene glycol) (PEG) solution with amino acid salts. In both cases almost equimolar absorption of CO₂ (1 mol CO₂ per mol of IL, or per mol of amino acid in PEG) was obtained.

In this work, the non-aqueous solvent PEG 200 was combined with short-chain amine group salts to increase CO₂ dissolution, and semiconductor nanoparticles were employed to initiate light-induced CO₂ reduction. For these studies, electron paramagnetic resonance (EPR) spectroscopy was used as a tool for examining the initial photo-induced charge separation and transfer in the presence of dissolved/grafted CO₂.

EXPERIMENTAL

Materials

All chemicals were of analytical grade and used as received, without further purification. Poly(ethylene glycol) 200 was purchased from J. T. Baker, carboxy-PEG₄-amine, C₁₁H₂₃O₆N, abbreviated in the text as CA(PEG)₄, from Thermo Scientific, tetra(*n*-butyl)ammonium hexafluorophosphate, Bu₄NPF₆, from Aldrich, anatase nanoparticles (*d* = 20 nm) from SkySpring, and Cu₂O colloidal nanoparticle (*d* = 30 nm) solution in ethanol from Aldrich. Research-grade carbon dioxide, 99.999 % (Airgas), was passed consecutively through two hydrocarbon traps (Supelco) to remove even trace amounts of impurities.

Instrumentation

X-Band continuous wave EPR experiments were conducted on a Bruker Eleksys E580 spectrometer equipped with an Oxford CF935 helium flow cryostat with an ITC-5025 temperature controller. The EPR spectra of the photogenerated charges were recorded at cryogenic temperatures from 4.5 to 77 K. The *g* factors were calibrated for homogeneity and accuracy by comparison with a coal standard, *g* = 2.00285 ± 0.00005. Simulations were performed using Bruker SimFonia, version 1.25. Samples in the EPR cavity were illuminated

using a 300-W Xe lamp (ILC) with water as the cut-off IR filter. Cyclic voltammetry measurements were performed with a three-component system containing a glassy carbon working electrode, Pt as the counter electrode, and Ag/AgCl as the reference electrode, using a BAS-100B/W (Bioanalytical Systems, USA) workstation with a single compartment closed quartz cell. Absorption spectra were recorded on a Shimadzu UV-1601 spectrophotometer.

RESULTS AND DISCUSSION

Electrocatalytic reduction of CO₂ in non-aqueous media has recently gathered increased interest,¹⁸ while semiconductor-assisted photocatalytic reduction is mainly focused on metal oxides in aqueous media. In photocatalytic processes, semiconductor metal oxide nanoparticles are used as light-harvesting materials. Nanocrystalline semiconductors are capable of coupling single photon events to the accumulation of multiple redox equivalents (photogenerated electrons) that participate in catalytic reduction of CO₂. The semiconductors Cu₂O (p-type), because of its favorable electronic properties for CO₂ reduction, Fig. 1, and TiO₂, because of its proven ability to convert carbon dioxide to methane in the presence of proton donors,^{7–11} were chosen as photocatalysts of interest. The low yield of methane production in aqueous solutions is due to the competition of water and

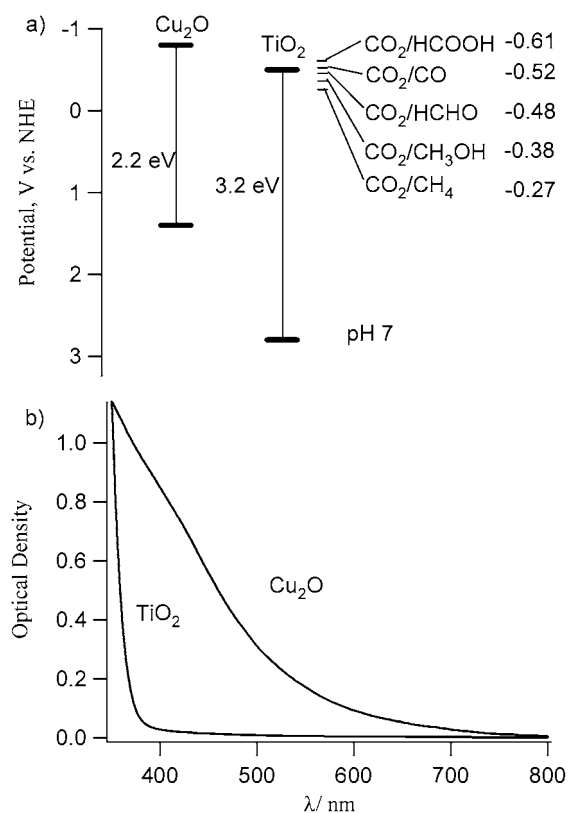


Fig. 1. a) Schematic presentation of the band positions and band gap energies and b) absorption spectra of Cu₂O and TiO₂ semiconductor nanoparticles. Optical pathlength: 0.5 cm.

carbon dioxide for the photogenerated electrons combined with the low solubility of carbon dioxide in water. Thus, the highest yields were achieved using a CO₂/water vapor (2:1) combination.¹¹ The redox potentials of CO₂ reduction products in aqueous solution are also indicated in Fig. 1a. In the absence of proton donors (as in non-aqueous solvents), the major product is carbon monoxide.

In order to increase the solubility of CO₂, 10 mM carboxy-PEG₄-amine, CA(PEG)₄ in PEG 200 solvent was used. The choice of CA(PEG)₄ was based on its high solubility in PEG 200 and because the amine group can effectively graft CO₂. It was shown previously that amino and amine groups capture CO₂ *via* the sequestration formation of the carbamic acid or carbamate pathways in a high yield.¹⁷ In order to gain insight into the photocatalytic reduction of CO₂ in non-aqueous media, photo-induced charge formation, separation and transfer in semiconductor nanoparticles were examined in CA(PEG)₄/PEG 200 solution saturated with N₂ or CO₂.

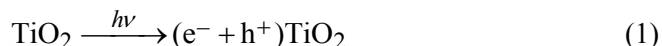
CO₂ in non-aqueous amine solution

The ability of CA(PEG)₄ dissolved in PEG 200 to sequester CO₂ efficiently was demonstrated using cyclic voltammetry. The voltammograms of the solutions saturated with N₂ and CO₂ are presented in Fig. 2a, from which it can be seen that the reversible one-electron redox process of CA(PEG)₄ with $E_{1/2} = -0.84$ V vs. Ag/AgCl occurred in the absence of CO₂. At the same time, when solution was bubbled with CO₂, a quasi-reversible electron transfer occurred. Moreover, the reduction of amine-grafted CO₂ starts at a potential of -0.5 V, while the electrochemical reduction of CO₂ occurs at rather negative potentials (more negative than -2 V) at low temperatures in most organic solvents. In the absence of CA(PEG)₄, no significant changes in the voltammograms of PEG 200 with and without CO₂ could be observed, Fig. 2b, showing that CO₂ does not dissolve in PEG 200 very efficiently, and confirming that the $-NH_2$ group is essential for the dissolving/grafting of CO₂.

Not only the increased solubility, but also the measured relatively positive potential for CO₂ reduction in this system made it the medium of choice for further studies and possible applications.

Light-induced charge transfer

The photo-excitation of TiO₂ (anatase) with energies greater than its band gap (3.2 eV) results in the formation of conduction band electrons and valence band holes (charge carriers):



EPR spectroscopy has been widely used to examine paramagnetic species in illuminated titania, starting with the seminal work of Howe and Gratzel.¹⁹ At cryo-

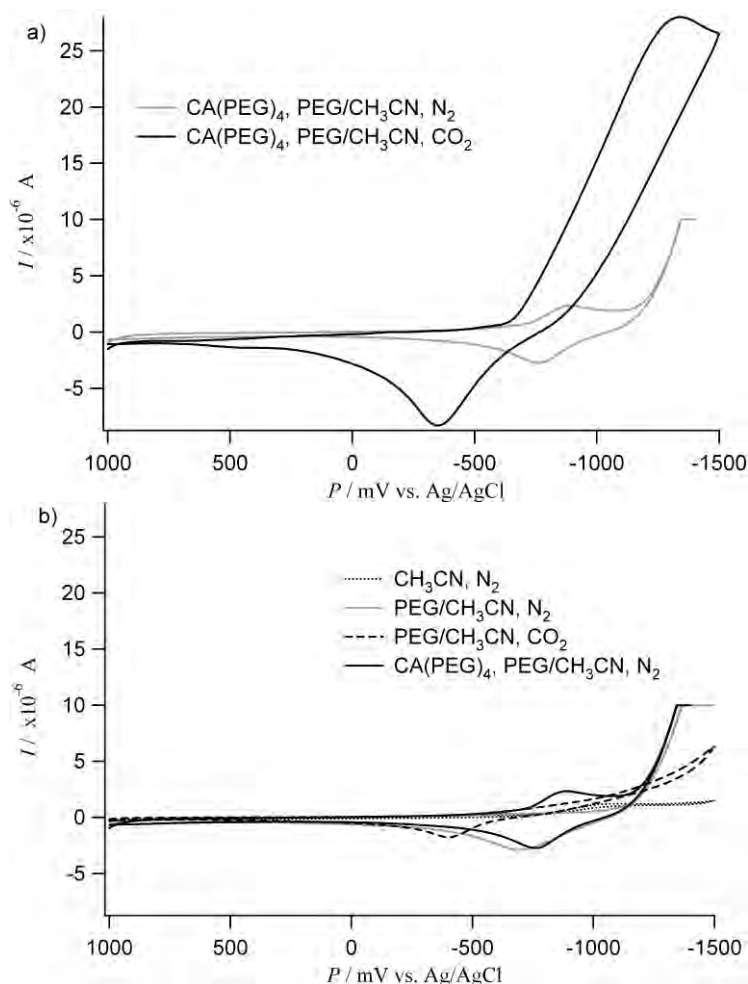


Fig. 2. Cyclic voltammograms of a) PEG 200 solutions containing 10 mM carboxy-PEG₄-amine, CA(PEG)₄, and 20 vol. % acetonitrile, saturated with N₂ and CO₂; b) solutions without CA(PEG)₄ measured as a control under the same conditions. All solutions contain 5 mM Bu₄NPF₆ as a redox relay. Glassy carbon as working, Pt as auxiliary and Ag/AgCl as reference electrodes were used. Scan rate 20 mV s⁻¹.

genic temperatures, photogenerated charge carriers localize in the interior of TiO₂ nanoparticles or migrate to the surface where they localize at surface trap sites. The signals associated with the trapped electrons are those due to lattice (Ti³⁺)_{latt}, sharp signal at $g_{\perp} = 1.990$ and $g_{\parallel} = 1.961$, and surface (Ti³⁺)_{surf} centers, broad signal with $g = 1.924$, Fig. 3a. The observed signals are characteristic of the electron in the Ti 3d orbital of the anatase lattice and surface.²⁰ Simultaneously, no signal due to the oxygen-centered radical, (Ti⁴⁺O[•])_{surf}, *i.e.* holes, was observed. The observed signal with $g = 2.001$ is due to the reaction of

photogenerated holes with carboxy-PEG₄-amine. The 6-line spectrum with the intensity ratios of 1:2:3:3:2:1 presented in Fig. 3b corresponds to CH₃CH₂[•] radicals,²¹ and is the result of C–O bond scission.²² The efficient scavenging of holes by carboxy-PEG₄-amine is facilitated by the strong binding of carboxyl groups on TiO₂.²³

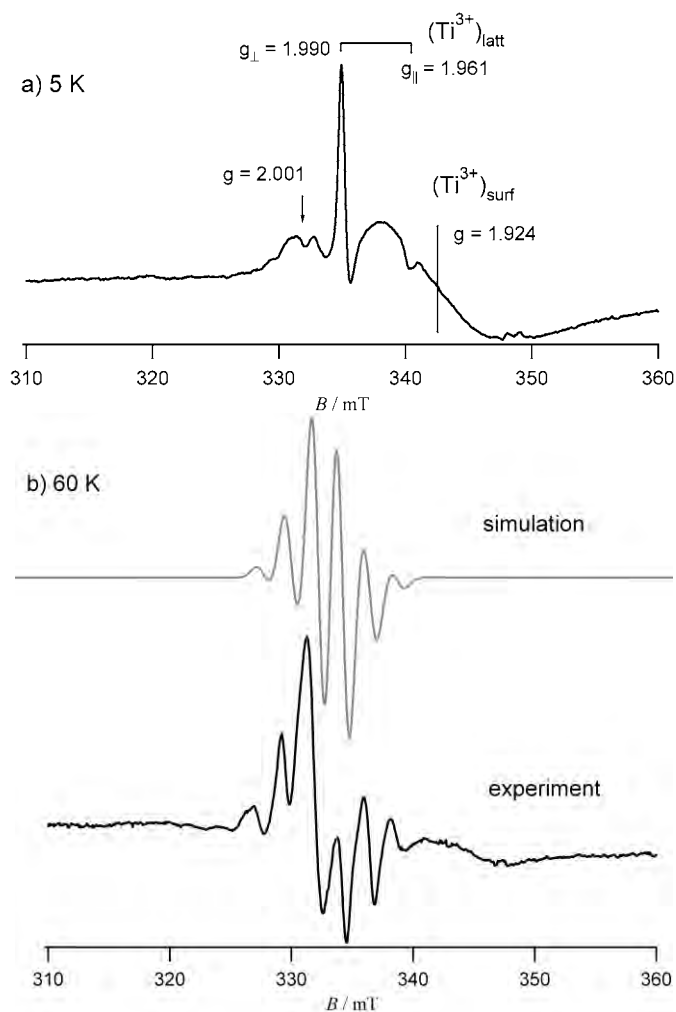


Fig. 3. EPR Spectra of TiO₂ in a solution of 10 mM carboxy-PEG₄-amine in PEG 200 measured under UV illumination at a) 5 K, power, 2 mW, modulation amplitude, 0.5 mT and b) 60 K, power, 0.2 mW, modulation amplitude, 0.3 mT. The gray line presents the simulated spectrum. The conditions of EPR measurements were adjusted to better resolve the signal from the CH₃CH₂[•] radical.

By increasing the temperature from 5 to 77 K, the electrons from the interior of the TiO₂ nanoparticle had enough energy to detrap and move to the surface where they localize at mid-gap states. The decrease of the signal for lattice-trapped and the increase of the signal that corresponds to the surface-trapped electrons, can be seen for a solution saturated with N₂, Fig. 4a.

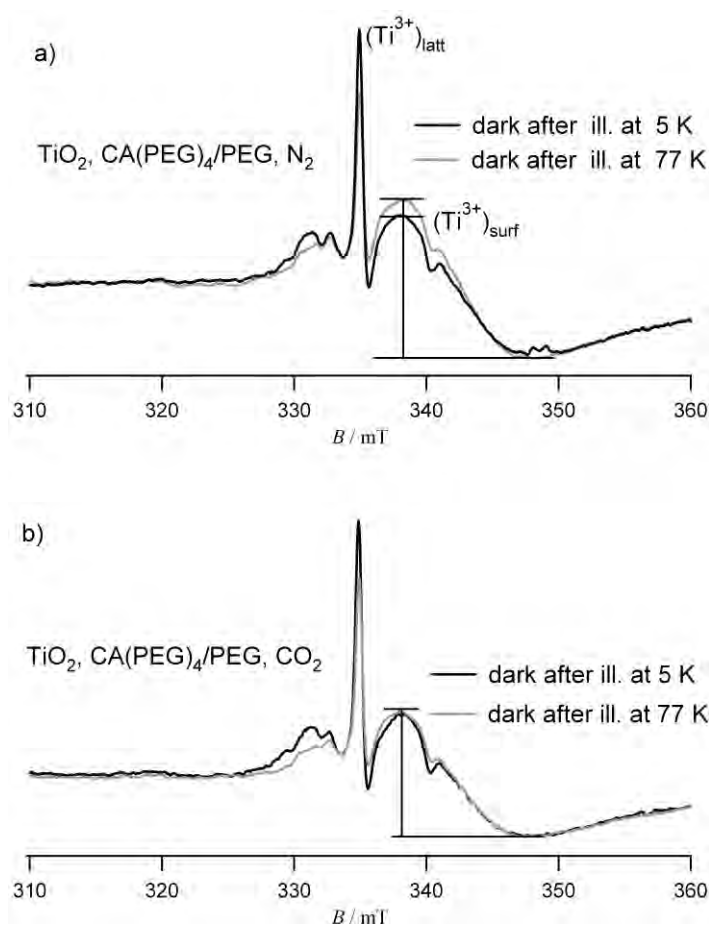
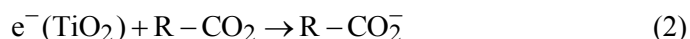


Fig. 4. EPR Spectra measured in the dark (at 5 K) after illumination at 5 and 77 K of a PEG 200 solution containing 10 mM carboxy-PEG₄-amine, CA(PEG)₄, and TiO₂ saturated with a) N₂ and b) CO₂. Power, 2 mW, modulation amplitude, 0.5 mT.

On the other hand, dissolved CO₂ acts as an electron acceptor, Eq. (2). The R-CO₂ in equations represents grafted CO₂, most probably carbamate:¹⁷



It was found that at the elevated temperature of 77 K, detrapped lattice electrons do not localize on the surface, rather they react with CO₂, Fig. 4b. Con-

sequently, no increase in the signal due to the surface-trapped electrons that were present at 5 K accompanies the decrease in the signal of the lattice-trapped electron. This means that *i*) the energy of mid-gap surface trapped electrons is below the redox potential for CO₂ reduction and *ii*) only conduction band electrons can react with CO₂. Although the driving force for CO₂ reduction with TiO₂ conduction band electrons is not high (Fig. 1), the efficient scavenging of photo-generated holes by CA(PEG)₄ enables a relatively high yield of the reduction reaction.

The conduction band electrons of cuprous oxide (Cu₂O) have a more negative potential than those of TiO₂; thus, the thermodynamic parameters favor reduction of CO₂. However, Cu⁺ is a non-paramagnetic ion and light-induced charge separation and transfer cannot be detected by EPR directly. As the Cu₂O nanoparticles used in this study did not have a protective ligand on their surface, a slow oxidation of bare nanoparticles occurred in air, resulting in the formation of thin layer of copper oxide (CuO) on the surface. This was confirmed by EPR spectra measured in the dark before illumination, Fig. 5. The spectra show hyperfine structure that is characteristic of Cu²⁺ ($I = 3/2$). In both cases (N₂ vs. CO₂ saturated solutions), the values of g_{\parallel} and g_{\perp} satisfy the relation $g_{\parallel} > g_{\perp} > g_e = 2.0023$ (g_e represents the g -tensor of free electron), indicating that the Cu²⁺ were coordinated by six ligand atoms in an axially distorted octahedron, that is characteristic of copper ions in CuO. However, the values for parallel and normal component differ, $g_{\parallel} = 2.256$ and $g_{\perp} = 2.036$ for N₂, and $g_{\parallel} = 2.276$ and $g_{\perp} = 2.038$ for CO₂, which suggests that CO₂ adsorbs/binds strongly to the surface of CuO,

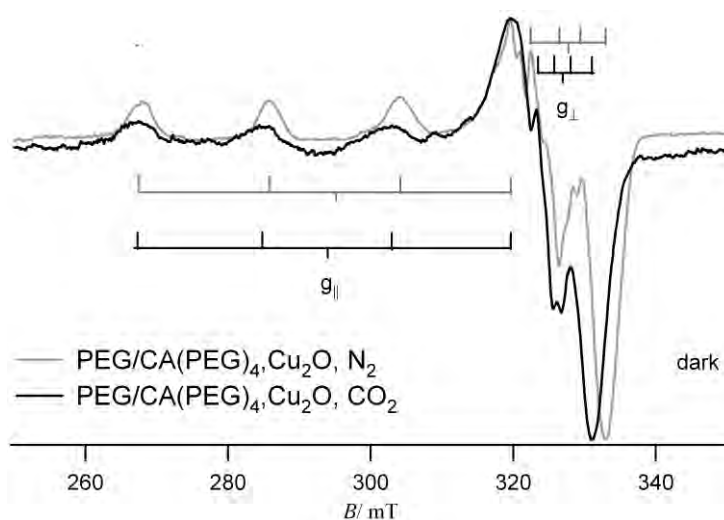
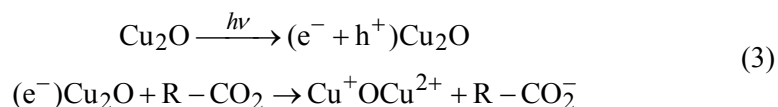


Fig. 5. EPR Spectra measured at 5 K in the dark of Cu₂O/CuO in PEG solution containing 10 mM carboxy-PEG₄-amine, CA(PEG)₄, saturated with N₂ or CO₂. Power, 2 m; modulation amplitude, 1 mT.

not only to carboxy-PEG₄-amine, affecting the hyperfine structure of surface Cu²⁺. The binding of CO₂ onto Cu₂O/CuO was previously observed in aqueous solutions.²⁴

Under illumination with visible light ($\lambda > 400$ nm), an increase in the concentration of Cu²⁺ was observed in the presence of CO₂, Fig. 6, due to electron transfer:



In the absence of CO₂, no change in the signal associated with Cu²⁺ was observed (Fig. 6a) because of the fast recombination of the photogenerated electrons and holes. The redox potential of valence band holes of Cu₂O is not

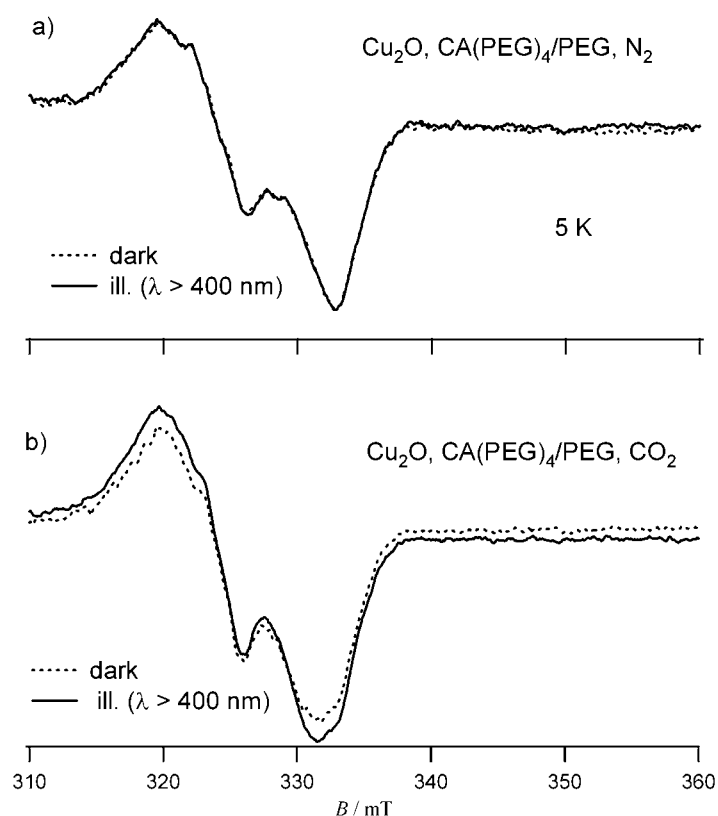


Fig. 6. EPR Spectra measured at 5 K in the dark and under illumination of Cu₂O/CuO in PEG solution containing 10 mM carboxy-PEG₄-amine, CA(PEG)₄, saturated with a) N₂ and b) CO₂. The magnetic field was centered on the normal component of the Cu²⁺ signal. Power, 2 mW; modulation amplitude, 1 mT.

positive enough to allow oxidation of carboxy-PEG₄-amine as no signals of organic radicals were observed in this system; thus, recombination of the charges was the favorable process. Therefore, the electron transfer from excited Cu₂O to CO₂ at the extremely low temperature of 5 K was due to the combined effects of the favorable redox potential of Cu₂O conduction band electrons and strong adsorption/binding of CO₂ on the nanoparticles.

CONCLUSION

Carboxy-PEG₄-amine, C₁₁H₂₃O₆N, when dissolved in poly(ethylene glycol) 200 efficiently sequesters CO₂. The grafting of CO₂ not only increases its solubility but enables reduction of CO₂ at a significantly more positive potential than the electrochemical reduction of CO₂ in most organic solvents or aqueous solutions. The efficiency of the one-electron transfer from photo-excited TiO₂ and Cu₂O nanoparticles to CO₂ was in the order Cu₂O > TiO₂, because of the preferential electronic and surface properties of the cuprous/cupric oxide nanoparticles.

Acknowledgment. This work was supported by the Department of Energy, Office of Science, Office of Basic Energy Sciences, under Contract No. DE-AC02-06CH11357.

ИЗВОД

ИСПИТИВАЊЕ ПРЕНОСА НАЕЛЕКТРИСАЊА У ЕКСЦИТОВАНИМ НАНОЧЕСТИЦАМА ЗА ФОТОКАТАЛИТИЧКУ РЕДУКЦИЈУ CO₂ У НЕВОДЕНОЈ СРЕДИНИ

НАДА М. ДИМИТРИЈЕВИЋ

Chemical Sciences and Engineering Division, and Nanoscience and Technology Division, Argonne National Laboratory 9700 S. Cass Ave., Argonne, IL 60439, USA

Раздвајање наелектрисања у побудјеним CO₂ и Cu₂O полупроводничким наночестицама је испитивано електронском парамагнетном резонантном спектроскопијом да би се добиле информације о фотокаталитичкој редукцији CO₂ у неводеној средини. Да би повећали растворљивост и везивање CO₂ користили смо карбоксил-PEG₄-амин у полиетилен гликолу 200 као растварачу. Нађено је да у том раствору редукција CO₂ почиње на потенцијалу од -0,5 V према Ag/AgCl, што је значајно позитивније него електрохемијска редукција у већини органских растварача и води (-2,0 V према Ag/AgCl). Ефикасност преноса електрона са побуђених наночестица на CO₂ зависи од термодинамичких и кинетичких параметара, наиме зависи и од потенцијала електрона у проводној траци и од адсорпције/везивања CO₂ на површину наночестица.

(Примљено 27. јула, ревидирано 19. септембра 2013)

REFERENCES

1. J. T. Kiehl, K. E. Trenberth, *Bull. Am. Meteorol. Soc.* **78** (1997) 197
2. D. H. Gibson, *Chem. Rev.* **96** (1996) 2063
3. X. Yin, J. R. Moss, *Coord. Chem. Rev.* **181** (1999) 27
4. M. Shi, Y. M. Shen, *Curr. Org. Chem.* **7** (2003) 737
5. S. Zhang, Y. Chen, F. Li, X. Lu, W. Dai, R. Mori, *Catal. Today* **115** (2006) 61
6. J. Huang, T. Ruther, *Aust. J. Chem.* **62** (2009) 298

7. T. Inoue, S. Fujishima, S. Konishi, K. Honda, *Nature* **277** (1979) 637
8. G. Li, S. Ciston, Z. V. Saponjic, L. Chen, N. M. Dimitrijevic, T. Rajh, K. A. Gray, *J. Catal.* **253** (2008) 105
9. B. Vijayan, N. M. Dimitrijevic, T. Rajh, K. A. Gray, *J. Phys. Chem., C* **114** (2010) 12994
10. K. Mori, H. Yamashita, M. Anpo, *RSC Adv.* **2** (2012) 3165
11. N. M. Dimitrijevic, B. Vijayan, O. G. Poluektov, T. Rajh, K. A. Gray, H. He, P. Zapol, *J. Am. Chem. Soc.* **133** (2011) 3964
12. a) P. G. Jessop, D. J. Heldebrant, X. W. Li, C. A. Eckert, C. L. Liotta, *Nature* **436** (2005) 1102; b) P. G. Jessop, S. M. Mercera, D. J. Heldebrant, *Energy Environ. Sci.* **5** (2012) 7240
13. a) C. M. Wang, H. M. Luo, D. Jiang, H. R. Li, S. Dai, *Angew. Chem. Int. Ed.* **122** (2010) 6114; b) C. M. Wang, X. Y. Luo, H. M. Luo, D. Jiang, H. R. Li, S. Dai, *Angew. Chem. Int. Ed.* **123** (2011) 5020
14. J. Im, S. Y. Hong, Y. Cheon, J. Lee, J. S. Lee, H. S. Kim, M. Cheong, H. Park, *Energy Environ. Sci.* **4** (2011) 4284
15. L. J. Hounjet, C. B. Caputo, D. W. Stephan, *Angew. Chem. Int. Ed.* **51** (2012) 4714
16. B. F. Goodrich, E. A. Price, W. F. Schneider, J. F. Brennecke, *J. Am. Chem. Soc.* **132** (2010) 2116
17. A.-H. Liu, R. Ma, C. Song, Z.-Z. Yang, A. Yu, Y. Cai, L.-N. He, Y.-N. Zhao, B. Yu, Q.-W. Song, *Angew. Chem. Int. Ed.* **51** (2012) 11306
18. L. L. Snuffin, L. W. Whaley, L. Yu, *J. Electrochem. Soc.* **158** (2011) F115
19. a) R. F. Howe, M. Gratzel, *J. Phys. Chem.* **89** (1985) 4495; b) R. F. Howe, M. Gratzel, *J. Phys. Chem.* **91** (1987) 3906
20. N. M. Dimitrijevic, Z. V. Saponjic, B. M. Rabatic, O. G. Poluektov, T. Rajh, *J. Phys. Chem., C* **111** (2007) 14597
21. R. W. Fessenden, R. H. Schuler, *J. Chem. Phys.* **39** (1963) 2147
22. Y. S. Won, D. Cho, Y. Kim, J. Lee, S. S. Park, *J. Appl. Polym. Sci.* **117** (2010) 2083
23. B. O'Regan, M. Gratzel, *Nature* **353** (1991) 737
24. G. Li, N. M. Dimitrijevic, L. Chen, T. Rajh, K. A. Gray, *J. Phys. Chem., C* **112** (2008) 19040.